Energy and Buildings 49 (2012) 335–347

Contents lists available at SciVerse ScienceDirect

Energy and Buildings

journal homepage: www.elsevier.com/locate/enbuild

Evaluation of energy supply and demand in solar neighborhood

Caroline Hachem [a,*], Andreas Athienitis [b], Paul Fazio [c]

[a] Department of Building Civil and Environmental Engineering (BCEE), Concordia University, 1455 de Maisonneuve Blvd., H3G 1M8 West Montreal, Quebec, Canada
[b] Department of Building Civil and Environmental Engineering, Concordia University, West Montreal, Quebec, Canada
[c] Building Envelope Performance Laboratory, Centre for Building Studies, Department of Building Civil and Environmental Engineering, Concordia University, West Montreal, Quebec, Canada

ARTICLE INFO

Article history:
Received 17 October 2011
Received in revised form 14 February 2012
Accepted 17 February 2012

Keywords:
Solar irradiation
Solar energy
Building integrated photovoltaic system
Electricity generation
Energy consumption
Neighborhood design
Geometrical shape density

ABSTRACT

The paper presents a study of solar electricity generation and energy demand for heating and cooling of housing units' assemblages. Two-story single family housing units, located in northern mid-latitude climate are considered in the study. Parameters studied include geometric shapes of individual units, their density in a neighborhood, and the site layout. The plan shapes of the housing units included in this study are rectangles and several variants of L shape. Site layouts studied are characterized by a straight road, a south-facing or a north-facing semi-circular road. Rectangular units and a site layout with straight road serve as reference for evaluating the effect of shape and site parameters. Results indicate that a significant increase in total electricity generation (up to 33%) can be achieved by the building integrated photovoltaic (BIPV) systems of housing units of certain shape-site configurations, as compared to the reference. The energy load of a building is affected by its orientation and shape. Increased heating demand by L variants (by up to 8%) is more than offset by annual electricity production of their BIPV systems (by up to 35%). Heating and cooling loads depend significantly on unit density in a site; Attached units require up to 30% less cooling and 50% less heating than detached configurations of the same site. Variation of surface orientation, particularly in curved site layouts, enables the spread of peak electricity generation over up to 6 h. This effect may be beneficial to grid supply efficiency. Energy balance assessment indicates that some unit shapes generate up to 96% of their total energy use. Neighborhood configurations studied generate between 65% and 85% of their total energy demand.

1. Introduction

The design of net zero energy solar buildings involves a two-fold approach of enhancing energy efficiency while optimizing active solar energy production using photovoltaics and thermal collectors. A net zero energy house (NZEH) generates as much energy as its overall energy consumption, over a typical year [1]. The net zero energy balance can be estimated based on on-site energy consumption or source energy consumption [2]. A successful methodology that may lead to net zero energy status depends upon selecting suitable technical strategies that respond to defined objectives in a specific context [3]. This paper considers the on-site energy consumption.

Coupling energy efficiency measures with active energy production techniques, such as photovoltaic and solar thermal collectors, enables the transformation of buildings into zero-energy systems or even net energy generating systems.

Reduction of energy consumption can be achieved through several measures, such as airtight, well insulated building envelope, implementation of HVAC efficiency measures, including the use of heat pumps, combined with geothermal energy or solar collectors, and finally the use of energy efficient appliances. Window properties and size, especially on the equatorial facade, can maximize passive heating. Solar heat gains can reduce significantly purchased heating energy. A well designed passive-solar building may provide 45–100% of daily heating requirements [4].

Near-equatorial facing roof surfaces are considered optimal for capture of solar energy for electricity and heat generation, and therefore for the integration of photovoltaic/thermal systems. In Canada, building integrated photovoltaic (BIPV) technology is estimated to be potentially capable of providing up to 46% of total energy demand of the residential need [5]. This figure is determined based on a conservative methodology which estimates the available area of roofs and facades for integration of grid connected PV systems, while accounting for architectural and solar constraints [6].

* Corresponding author. Tel.: +1 514 8482424x7080; fax: +1 514 848 7965.
E-mail addresses: c_hachem@encs.concordia.ca, carolinehachem@gmail.com (C. Hachem).

0378-7788/$ – see front matter © 2012 Elsevier B.V. All rights reserved.
doi:10.1016/j.enbuild.2012.02.021

The performance of a PV system depends mainly on the tilt angle and azimuth of the collectors, local climatic conditions, the collector efficiency, and the operating temperature of the cells. During the winter months, the insolation can be maximized by using a surface tilt angle that exceeds the latitude of the location by 10–15°. In summer an inclination of 10–15° less than the site latitude maximizes the insolation [7]. The PV system is commonly mounted at an angle equal to the latitude of the location, to reach a balance between winter and summer production [8–10].

Building shape plays an important role in governing energy consumption in buildings, as well as having a significant effect on thermal performance and capture of solar energy [11,12]. Rectangular shape is generally considered as optimal for passive solar design and for energy efficiency [13]. However, under certain design conditions in urban context, this shape may not be optimal [12]. For instance, rectangular house plan does not allow uniform penetration of daylight, especially to the north part of the house, where minimum windows are suggested for northern climates. Furthermore, it should be born in mind that shape design is governed by many constraints other than energy efficiency, such as functional demands and quality of life of occupants. For these reasons it is important to explore the penalties, as well as the benefits associated with plan layouts other than rectangular, and with different roof geometries.

Design of solar neighborhoods for exploitation of solar radiation for passive heating, for improved daylight, and for electricity generation, involves consideration of key parameters, including, in addition to building shapes, their density within a site, and the site layout.

Spatial characteristics of neighborhoods and land use regulations can significantly affect solar potential and energy demand of buildings. Land-use patterns influence local temperature distributions [14]. High density development reduces cost and energy use, on one hand while reducing solar accessibility, on the other [15]. Site shape and layout of streets within this site can determine orientation of buildings and thus influence their accessibility to solar radiation [16].

Several studies have focused on investigating the distribution of solar radiation on different surfaces in a built environment, as well as on the availability of solar energy and its optimization, at the urban scale [e.g. 17,18,19]. Compagnon [20] proposed a methodology for estimating the amount of solar energy available to a building of any shape, taking into account obstructions due to the surrounding landscape and associated reflections. Kampf et al. [21] have developed a methodology, employing a multi objective evolutionary algorithm, to minimize energy demand of buildings in an urban area and to maximize incident solar irradiation whilst accounting for thermal losses.

Notwithstanding the interest in the effect of urban development on solar energy, and the various investigations conducted to optimize solar energy, several aspects are not sufficiently addressed. The study presented in this paper forms part of an ongoing research into the effects of certain design parameters of residential neighborhoods on their solar potential and energy performance [11,12,22]. The current study presents an investigation of the electricity generation potential by building-integrated photovoltaic system, and of the energy demand of two-storey single family housing unit assemblages. Climatic data of Montreal, Canada (45°N), serve as input for the analysis. The main objective is the evaluation of alternative patterns of neighborhood to achieve potential net zero energy communities. The main parameters employed in neighborhood design included in this investigation are the shape and orientation of individual units, the density of units in a site, and the site layout.

2. Methodology and design approach

The research presented in this paper is divided into three main parts: (1) the analysis of electricity generation potential by neighborhoods, (2) the analysis of energy performance in terms of heating and cooling consumed by units and neighborhoods, and (3) comparison of energy production and energy consumption of individual units and of whole neighborhoods.

The analysis of electricity generation potential and of energy demand of housing units and neighborhoods is a parametric investigation, in which the effects of three main parameters are assessed. These parameters are the shape of individual units within a neighborhood, the density of units in the neighborhood and the over-all layout of the site in which the neighborhood is located.

The general characteristics of the investigated neighborhoods are based on various sources, including guidelines of urban design, street designs and zoning bylaws [e.g. 23,24,25]. Detailed description of the design of these neighborhoods can be found in Hachem et al. [22]. The design methodology consists of first determining the site layout, followed by design of unit shapes to conform to this layout, and finally combining the shapes in different configurations. For each site, several configurations consisting of combinations of groups of three to six units of a given shape are studied. For each site/shape combination, two densities are considered: medium-low density (around 7 units per acre (u/a)) of detached units [26] and medium-high density (ca. 16 u/a), consisting of attached units. The effect of higher density is studied through configurations of rows of housing units, with varying distance between rows. A maximum practical density of 35 u/a can be reached in some row configurations.

All configurations are subjected to simulations aimed at estimating the BIPV electricity generation and the heating and cooling loads. The simulation employs the EnergyPlus building simulation program [27]. The simulations are followed by a comparative analysis to assess the effect of shape, density and site layout on solar potential and energy performance, relative to a reference case. A rectangle, with aspect ratio of 1.3 and a hip roof serves as the shape reference. The aspect ratio is the ratio of the south-facing facade to the perpendicular facade, and a ratio of 1.3 is considered optimal for passive solar design in northern climate [28]. A site with units arranged along a straight road serves as the site layout reference. Details of the three studied parameters are presented below.

2.1. Characteristics of housing units

The studied housing units are two-storied with constant floor area of 60 m^2 (total livable area of 120 m^2). The two-storey housing option adopted in this study represents one of the most common types of single family homes in Canada [29]. The floor area is based on the need to reduce costs by having a compact design. It should be mentioned that the average floor area for Canadian household, including detached homes, row houses and apartments is 121 m^2, while the average area of single detached house is in the order of 140 m^2 [30].

Two basic shapes are employed – rectangle and L shape. Variations of L shapes are explored to identify design possibilities that enhance solar radiation capture potential on near-south facing roofs and facades. The characteristics of the housing units are detailed in Table 1. The basic design of the units relies on passive solar design principles [13] and rules of thumb [31]. The design ensures that the overall east–west dimension of all units – the solar facade, is larger than the perpendicular dimension (north–south), to maximize passive solar gains in winter. A geothermal heat pump with a coefficient of performance (COP) of 4 is assumed to supplement the passive and active solar heating systems. Ground source heat pumps (GSHPs) can supply heat of up to quadruple the energy

Table 1
Main characteristics and electric loads of housing units.

Thermal resistance values	Exterior wall: 6.6 RSI Roof: 10 RSI Slab on grade: 1.2 RSI
Thermal mass	20 cm ground floor concrete slab
Window type	Triple glazed, low-e, argon filled (SHGC = 0.57), 1.08 RSI
Area of south glazing as percentage of south-facing facades	35%
Shading strategy	Interior blinds
Occupants	2 adults and 2 children, occupied from 17:00–8:00
Set point temperatures	Heating set point 21 °C, cooling set point 25 °C
Infiltration rate	0.8 ACH @ 50 Pa
Assumptions for electrical loads	
Lighting	3 kWh/m^2/year (360 kWh) [33]
DHW	2.75 kWh/day/person [33]
Major appliances	1600 kWh/year [34]
Minor appliances	1100 kWh/year [36]

of the electricity they consume, by using ground extracted heat [32].

2.1.1. Lighting and appliance loads

Electrical loads for major and minor appliances, for lighting and for domestic hot water (DHW) are assumed based on a variety of sources dealing with the electrical load in energy efficient and net zero energy houses [e.g. 30,33,34]. Major appliances include refrigeration equipment (freezer and refrigerator), dishwasher, washing machine, clothes dryer and cooking appliances. Minor appliances include a wide range used in the kitchen and for entertainment purposes. These loads are summarized in Table 1. Lighting consumption can be limited to 3 kWh/m^2/year for a NZEH in mid-latitude locations, based on the assumption that a NZEH is expected to optimize daylight utilization [33].

Hot water energy consumption can be limited to a daily average of 2.75 kWh per occupant (Sartori et al, 2010), based on the assumption of hot water usage of 50 L/day/person. This value is derived from information provided in the literature (e.g. (66.6 L/person [35]) and the Canadian equilibrium initiative (56.25 L/person)), with the assumption that it is possible to reduce significantly the daily domestic hot water (DHW) consumption, using different methods (e.g., use of low-flow showerheads).

2.1.2. Shapes of housing units

Rectangle and L shape and its variations selected in this study can be considered as prototypes of convex and non-convex shapes for passive solar design. Other basic shapes can be derived from combination/variation of these shapes. The effect on solar potential of several additional shapes is presented in [11].

L shape consists of a main wing and an attached branch. The main wing is assumed to be oriented east–west, so as to have the long facade facing south. The ratio of the length of the branch to that of the main wing is termed the depth ratio – a/b in Table 2. The branch can be attached at either the west end, W configuration, or at the east end, E configuration. It can also be facing south (S) or north (N). Thus the configuration L-WS, for instance, denotes L shape with the branch attached to the west end of the main wing towards the south (see Table 2). The geometry of the basic L shape is characterized, in this study by a depth ratio (a/b) of 1/2. This ratio is selected in order to minimize the shade cast on the main wing, while maintaining a functional plan [11].

L variants are characterized, in addition to the depth ratio, by the angle β – the deviation from 90° of the angle enclosed between the main wing and the branch. Two values of β are considered in this study – 30° (enclosed angle 120°) and 60° (enclosed angle 150°). L variants are identified by the letter V followed by a series of characters specifying the position and angle of the branch (Table 2). An additional shape, termed hereunder obtuse-angle (denoted O) can be considered a special L variant with a larger value of the angle enclosed between the wings (160°, β = 70°). For obtuse-angle shape, the depth ratio has no significant effect, as the wings do not mutually shade. This shape is particularly suitable for curved site layouts. The obtuse-angle shape may be facing in a generally south direction – O-S or north direction – O-N.

2.1.3. Roof design

The basic roof design in this study is a hip roof with tilt and side angles of 45° (roofs with tilt and side angle variations are studied in [11,37]). The height of the lowest edge of the roof is kept constant at seven meters above ground level. The roof of the rectangular shape is designed with the ridge running east–west along the center of the plan area. In L shape and its variants the ridge of each wing runs along its center, with a triangular hip at the end of the branch and a gable at the free end of the main wing. Both wings of the obtuse-angle roof end with hips.

A photovoltaic system is assumed to cover the total area of all south and near-south facing roof surfaces. These surfaces include the triangular portions of hip roofs of L shape and its variants and the two near-south facing surfaces in obtuse-angle roofs. A BIPV system covering a complete roof surface may also be designed to act as the roof weather barrier in addition to producing electricity. Fig. 1 illustrates the integration of the PV systems in south and near-south facing roof surfaces, in shapes used in sites I, II and III (Fig. 2).

An additional roof, termed hereunder the optimum roof, is designed to be used as control for comparative evaluation of the electricity generation potential by the south-facing BIPV systems of all other roofs. The optimum roof is a gable roof with 45° tilt angle covering the rectangular shape.

2.2. Site layouts

Three site layouts are studied. Site layout I is characterized by a straight road. The other two layouts incorporate semi-circular roads. In site II the curved road is south-facing (i.e., the center lies south of the arc), while in site III it is north-facing. The circular road is selected to represent an extreme case of a curved road as, for instance, in a *cul-de-sac* street design. The housing units are positioned with respect to the shape of the roads, in both curved sites.

Two basic shapes of detached units are used in site I, rectangle and L-WS shapes (Fig. 2a). In addition, an L variant of β = 30° is studied – V-WS30.

Configurations of site II include rectangular shape, combination of L shape and its variants and a configuration of obtuse-angle shapes (Fig. 2b). In the last configuration (obtuse-angle) the two extreme units – U1 and U5 are L variants (V-ES60 and V-WS60), in an attempt to optimize facade orientation for insolation. Configurations of site III are mirror images of those of site II, relative to an east–west axis (Fig. 2c).

2.2.1. Density

Density is influenced by the spacing between units in a row (s) and by the spacing between rows of units (r) – three values of spacing are adopted for each site: s_1, the basic spacing of detached units, is assumed as 4 m in site I. The spacing between detached units in a curved site varies, depending on the curvature of the road and the shape of the units (Fig. 2). In a site with a curved road of 42 m diameter the basic spacing s_1 between rectangular units is assumed as 4 m. For L variant units it varies between 4 m and 7 m. In order to assess the influence of increased spacing on energy demand,

Table 2
Characteristics of L shapes and L variations.

Direction of L branch	Shape					
	L shape	Variations of L shape				
		L variant (V)				Obtuse angle
South	(L-WS)	$\beta = 60^\circ$ – West (V-WS60)	$\beta = 30^\circ$ – West (V-WS30)	$\beta = 30^\circ$ – East (V-ES30)	$\beta = 60^\circ$ – East (V-ES60)	(O-S)
North	(L-WN)	$\beta = 60^\circ$ – West (V-WN60)	$\beta = 30^\circ$ – West (V-WN30)	$\beta = 30^\circ$ – East (V-EN30)	$\beta = 60^\circ$ – East (V-EN60)	(O-N)

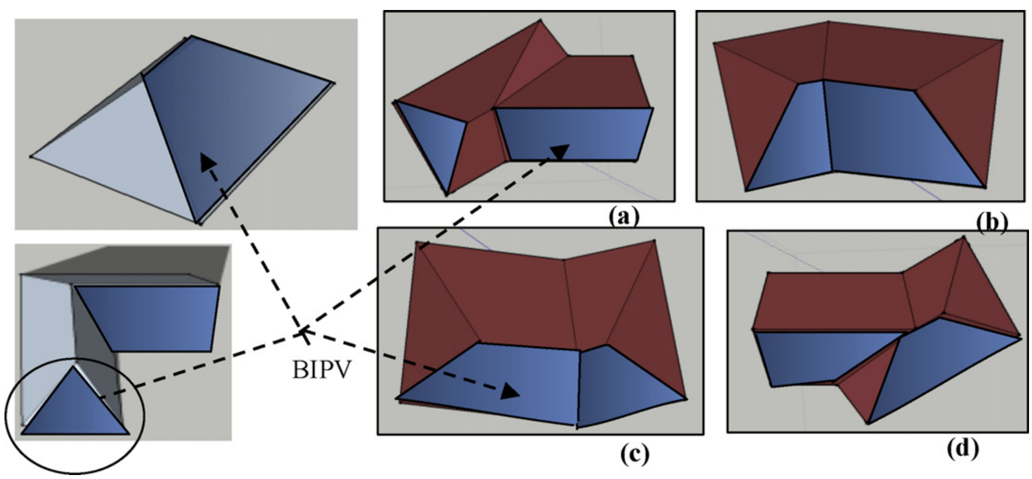

Fig. 1. Irregular roof shapes and PV integration. PV integrated surfaces are shown in gradient color. (a) and (b) represent roofs of V-WS60- variant and obtuse-angle O-S in site II, (c) and (d) represent the corresponding shapes in site III, V-EN60 and O-N.

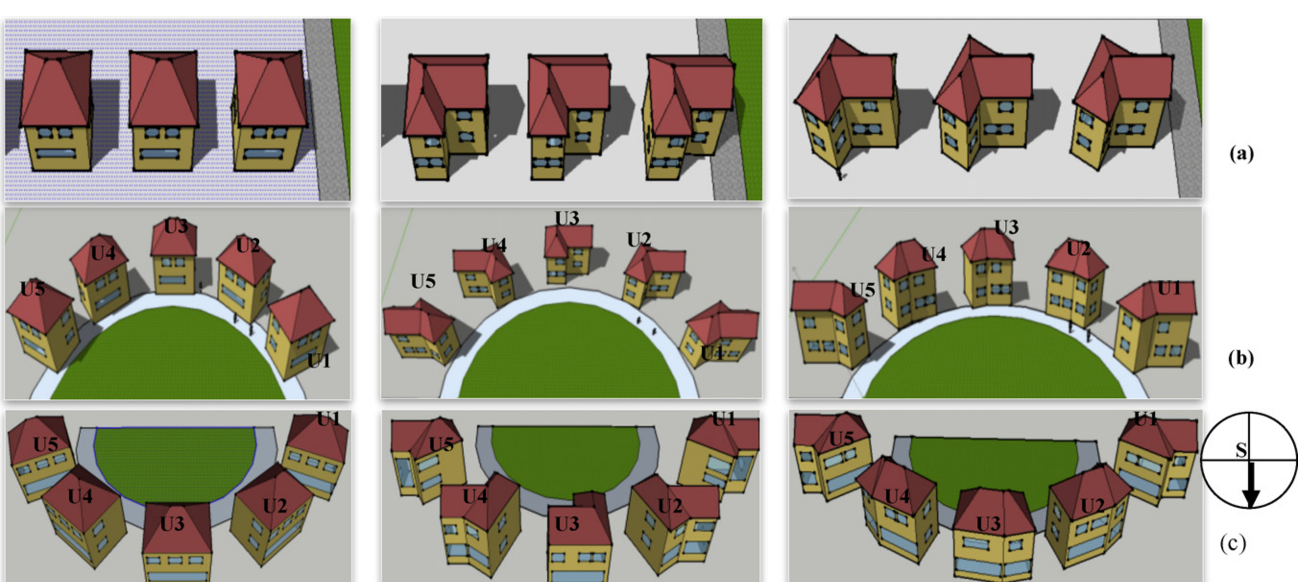

Fig. 2. Configurations of shapes used in different site layouts: (a) site layout I; (b) site layout II; (c) site layout III.

Table 3
Design parameters for the sites.

Parameters and values			
Shape	Site layout	Density	
		Spacing effect (s)	Row effect (r)
R – Rectangle/trapezoid L – L V – L variant O – Obtuse-angle	I – Straight II – Curved south, with diameter: $D1 = 42$ m (associated with s_1) $D2 = 52$ m (associated with s_2) III – Curved north ($D1$, $D2$)	$s_0 = 0$ (attached) $s_1 = 4$ m – site I, detached rectangles in sites II, III; 4 m – 7 m detached L variants in sites II, III $s_2 = 2s_1$	r_0 – no 2nd row $r_1 = 5$ m $r_2 = 10$ m $r_3 = 20$ m

a second spacing $s_2 = 2s_1$ is adopted. In a curved site this spacing corresponds to a road diameter of 52 m. At the other extreme, the highest density is obtained by attaching units in triplex, quadruplex or pentuplex configurations, with $s_0 = 0$. The neighborhood design parameters and their values are summarized in Table 3.

In site I the effect of obstructing the south facades of selected configurations by a row of similar housing configurations is assessed by what is termed hereunder row effect. The minimum distance between the two rows, to avoid shading, can be estimated based on the shadow length equation [38]:

$$SL = \frac{H\cos(\phi - \Psi)}{\tan\alpha} - \frac{W}{2} \quad (1)$$

where SL is the shadow length, H is the total height of the shading building, ϕ is the solar azimuth, ψ is the azimuth of the surface, α is the solar altitude, W is the width of the shading building.

Using the shadow length equation for the 21st December, associated with the lowest sun altitude at solar noon, the minimum spacing to avoid row shading is ca. 25 m. Therefore, to assess the effect of shading, three values of row spacing (r) are simulated: 5 m, 10 m and 20 m (Table 3). The studied configurations are the detached rectangular units and the detached and attached configurations of L variant (V-WS30) (Fig. 3). It should be noted that 5 m is unlikely to be employed when the south-facing facade is the principal facade and its inclusion in the study is aimed at providing an extreme case in order to assess the trend.

Attached configurations for sites II and III are shown in Fig. 4. Three shapes are employed in the configurations of each site – rectangular, L variants and obtuse-angle. The rectangular shape is replaced with a trapezoid, to allow attachment of units along the curve. The south-facing curve of site II implies that the narrower side of the trapezoid is south or near-south facing (see Fig. 4a), whereas for site III the wider side faces south (Fig. 4d). Non-trapezoid layouts include in addition to the four central attached units two detached units at the extremes of the curve for improved site design. These detached units are not included in the analysis for density effect.

2.3. Simulation modeling

EnergyPlus building simulation software [27] is employed in the simulations. SketchUp/OpenStudio [39] is employed to generate geometric data for EnergyPlus. Each housing unit is modeled as a single conditioned zone. The Conduction Finite Difference algorithm is selected as the heat balance algorithm. This solution technique employs a one-dimension finite difference method to represent the construction elements. A time step of 10 min is used in the simulations.

The main characteristics of the models employed by EnergyPlus are summarized below.

2.3.1. Weather data

This study is applied to Montreal, Canada (45°N latitude). The heating degree days (HDD) for Montreal are ca. 4519 HDD [40]. Two design days – a sunny cold winter day (WDD) (in January), and a sunny hot summer design day (SDD) (in July) – are selected. The daily average dry bulb temperature and total solar insolation are used as basis for the selection of these design days [41]. The main purpose of these design days is to explore the solar potential of all studied configurations, thus the WDD and SDD are selected to represent two extreme sunny days. Additionally, a whole year weather data set is used to estimate the annual electricity production potential of the PV system installed on south-facing roof surfaces (details are given below).

The weather files of EnergyPlus are used for the simulations [42]. The weather data file, which is based on CWEC – Canadian weather for energy calculations – provides hourly weather observations. These observations simulate a one-year period, specifically intended for building energy calculations. The data collected for this typical year includes hourly values for solar radiation, ambient temperature, wind speed, wet bulb temperature, wind direction and cloud cover.

2.3.2. EnergyPlus solar radiation computations

The instantaneous solar radiation accounts for direct beam and diffuse radiation, as well as for radiation reflected from the ground and adjacent surfaces. The solar model used in this study employs the ASHRAE clear sky model [43]. This model is the default model used by EnergyPlus to estimate the hourly clear-day solar radiation for any month of the year.

Validation tests show that the simulation codes used in EnergyPlus (in addition to other simulation programs such as ESP-r) are capable of computing total irradiated solar energy on building facades with a high precision for long time periods (such as months) [44]. Heat flow through windows was also shown to be predicted by EnergyPlus with good precision, where the difference with the experimental data was in the order of 5.8% [45].

To study the solar radiation incident on different shapes it is necessary to determine the shaded surfaces of a building, as well as surfaces that are directly reached by solar irradiation. The shading algorithm accounts for self-shading geometries, such as L shape.

2.3.3. Slab on grade modeling

The slab program [27] is used to compute the temperature of the underside surface of the slab (in contact with the ground). Taking into account the slab and ground properties, the slab program produces average monthly temperature of the slab, which is input in EnergyPlus to carry out the simulations.

2.3.4. BIPV modeling

The TRNSYS PV model (or equivalent one-diode model), provided by EnergyPlus is selected to perform electricity generation simulations of the BIPV systems. The TRNSYS model employs a four-parameter empirical model to predict the electrical performance of PV modules. This model is detailed in [7].

The current–voltage characteristics of the diode depend on the PV cell's temperature. The model automatically calculates parameter values from input data, including short-circuit current,

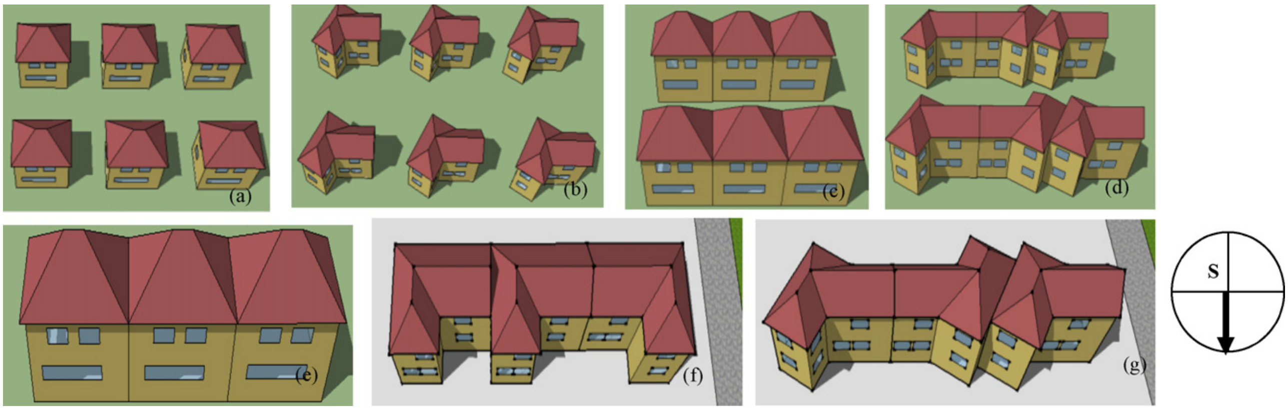

Fig. 3. Site I density effects: (a) row effect, rectangular units; (b) row effect, detached L variant; (c) row effect, attached rectangles; (d) row effect, attached L variant; (e) Attached rectangles; (f) attached (triplex) L–S shapes; (g) attached L variants ($\beta = 30^\circ$).

open-circuit voltage, current at maximum power [46]. For this study, the PV array is selected from EnergyPlus database to provide approximately 12.5% efficiency, under standard conditions. The cell temperature under standard conditions is considered as 25 °C and the reference insolation is set at 1000 W/m^2. The electrical conversion efficiency decreases by some 0.45% for each °C increase of cell temperature from the temperature under standard conditions. For Montreal, the annual potential of PV electricity generation of south-facing surfaces at latitude tilt angle is about 1200 kWh/kW$_{peak}$ of installed PV [47].

3. Presentation and analysis of results

3.1. Electricity generation potential

Electricity generation potential of a BIPV system depends on three main factors: area of available surface for the PV integration, its azimuth angle (or orientation relative to south) and the shade cast on the surface. Roof tilt angle is an important factor but it is assumed constant in this study. The other two roof factors – area and azimuth angle, are defined by the shape of the housing unit. For an assemblage of units in a specific neighborhood pattern, the BIPV systems can be shaded by adjacent units, and orientation can be dictated by the site layout, as for example in site II and site III. The main effects of housing unit shape, their density within a site and the site layout on the electricity generation of BIPV systems are summarized below. A detailed study of these effects is presented in [22].

3.1.1. Effect of shape

The annual electricity generated by the BIPV of south and near-south facing roof surfaces of isolated units of each shape is presented in Fig. 5 (refer also to Fig. 2 for the relevant shapes). It should be noted that in site II rectangle, L and V-WS30 shapes are identical with those of site I while in site III shapes other than rectangle are the mirror image of these used in site II (see Table 1). The annual electricity generation of isolated units of each shape is compared to the reference case and to the optimal roof (rectangle with a gable roof) in Table 4. The main observations of the shape effect on electricity generation for sites I, II and III are as follows:

- The shade on the south-facing roof in all non-convex shapes is mitigated by a small depth ratio as well as by increased angle between the wings. Consequently the electricity generation potential in such units is not significantly affected by shading.

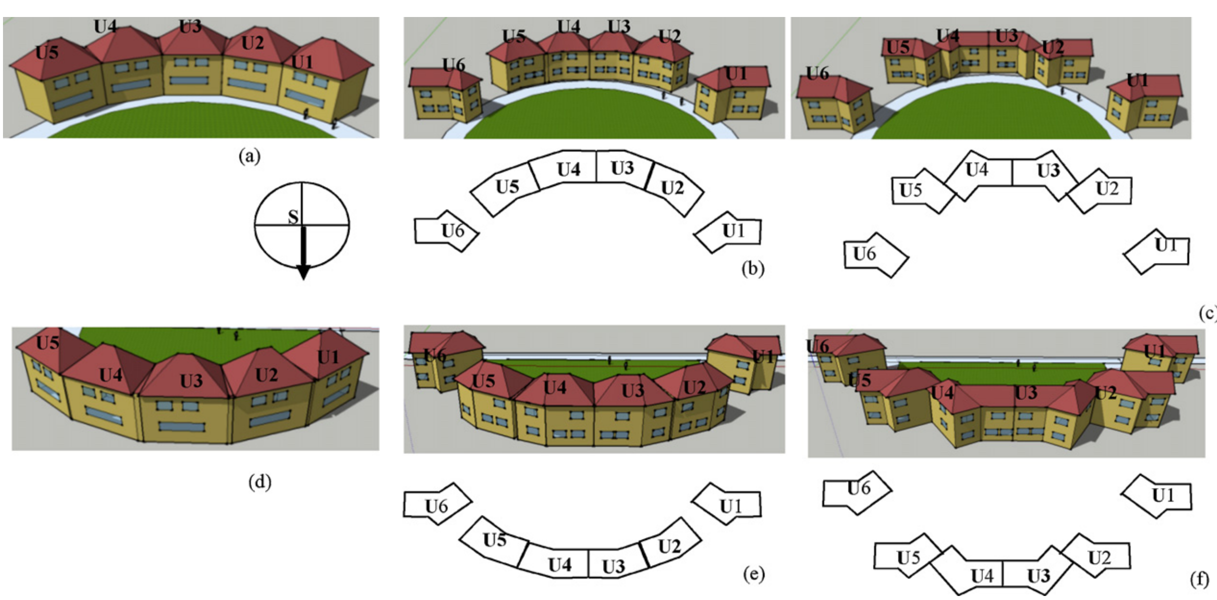

Fig. 4. Attached units in sites II and III. Site II: (a) trapezoid; (b) obtuse-angle; (c) L variants. Site III: (d) trapezoid; (e) obtuse-angle; (f) L variants.

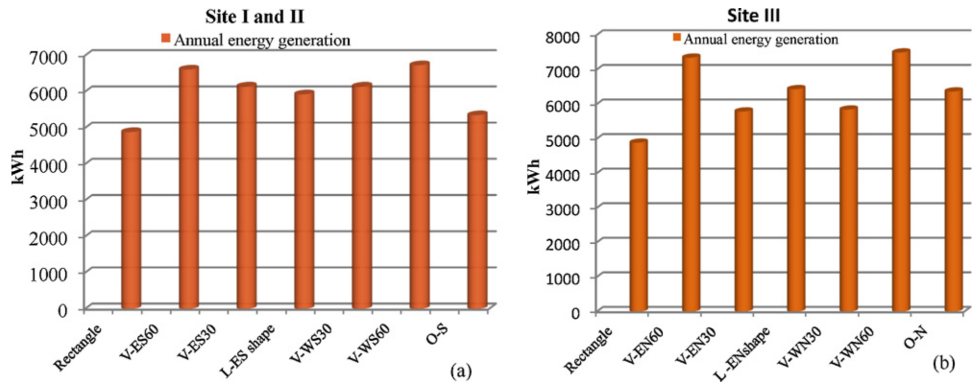

Fig. 5. Annual energy production of isolated units in (a) site I and II (identical units are used in site I and II), (b) site III.

- The L and L variant shapes provide larger roof area, than the reference case (rectangle with a hip roof) and therefore an increase in annual electricity generation (up to 38% increase). In site III, the increase in total annual generation of some units, relative to the reference, can reach 53% (units of V-WN60 shapes). Obtuse-angle shape in site III generate up to 30% more electricity annually than the reference.

3.1.2. *Effect of density*

The effect of density on electricity generation by roofs is expressed as the difference between the average electricity generation of attached and detached configurations of units of the same shape in a given site. The analysis is performed for the design days as well as for annual production. The average generation is of particular interest in a neighborhood design, since it gives an insight of the potential of an assemblage of units to generate electricity.

3.1.3. *Effect of spacing*

The results for site I indicate that there is no significant difference in electricity generation between attached and detached configurations of a given shape. A maximum reduction of 3% or less of the average annual generation is observed in the attached units of L shape due to mutual shadings between units. For sites II and III, the main results are summarized as follows:

- The reduced south-facing roof area of the trapezoid roof of attached units in site II, as compared to the rectangular shape of detached units, results in reduction of the average annual electricity generation by up to 10%. In site III there is an increase of similar magnitude, due to the increased roof surface area.
- No significant difference is observed for site II between the annual energy production of the detached and attached configurations of L variants and obtuse-angle shapes.
- For site III, the attached configurations of both L variants and obtuse-angle perform better than the corresponding detached configuration (10% difference for L variants, and 3% for obtuse-angle).

3.1.4. *Row study*

The row effect is measured by comparing the electricity generation of the roofs of the obstructed row to that of the exposed row. The results show that for a row separation of 5 m the electricity generation of the rectangular unit is reduced by a maximum of 7% for the WDD. No shadowing effect on electricity generation is observed for row separation larger than 5 m.

3.1.5. *Effect of site layout*

Site layouts are compared for the two shapes shared by all sites–rectangles and L variants. The comparison of the total annual generation averaged per unit of site II and site III to the corresponding configurations of site I, which serves as reference, indicates an increase of 6% and 9% for the attached L variant configuration in site II and site III respectively. A maximum reduction of about 3% is observed in the generation of the detached rectangle configuration in site II and site III as compared with the similar configuration in site I.

3.1.6. *Shift of peak electricity generation*

An important result of the interaction of site layout and units configurations is the shift of peak electricity generation among units in the neighborhood. A maximum shift of 3 h is obtained in the electricity produced by BIPV systems of different roof surfaces of units of site I. In site II the rotation of whole units in addition to the rotation of individual surfaces produces a difference in peak time of up to 6 h for the WDD. Fig. 6 presents the daily variation of electricity generation of configurations of site II for a WDD. Similar results are obtained in site III.

3.2. *Energy consumption for heating and cooling*

3.2.1. *Effect of shape on energy demand*

The annual heating and cooling loads for rectangular units are determined as function of their rotation from due south. The results indicate that both heating and cooling loads increase with increased angles of rotation. Heating loads are converted to electricity consumption using a COP of 4, associated with a typical geothermal heat pump. Total annual energy use for heating and cooling of rectangular units at different orientations is presented in Fig. 7. The

Table 4
Comparison of annual electricity generation of all housing units to the optimal case and to the reference case.

Sites I and II	Rectangle	V-ES60	V-ES30	L-ES	V-WS30	V-WS60	O-S
Comparison to gable	0.65	0.87	0.81	0.78	0.81	0.89	0.71
Comparison to reference	1	1.35	1.26	1.21	1.26	1.38	1.10
Site III	Rectangle	V-EN60	V-EN30	L-EN	V-WN30	V-WN60	O-N
Comparison to gable	0.65	0.97	0.77	0.85	0.77	0.99	0.84
Comparison to reference	1	1.50	1.18	1.32	1.18	1.53	1.30

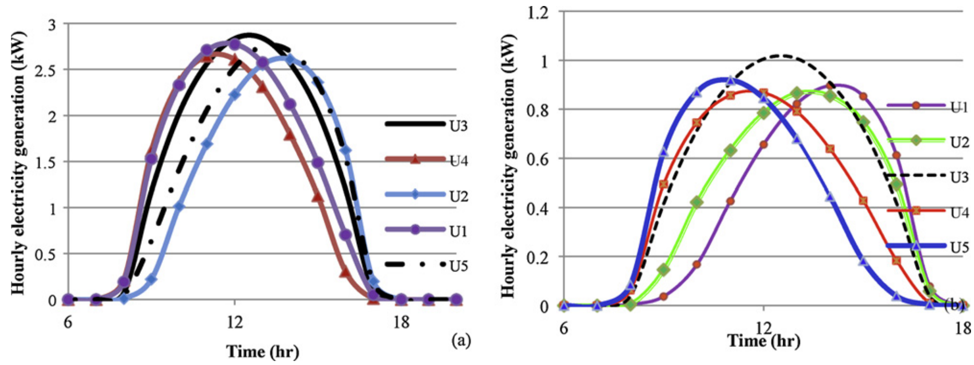

Fig. 6. Hourly electricity generation (from 6 a.m. to 6 p.m.) (kW) for detached units of site II for the WDD: (a) on the total south roof rectangular shape (26 m^2 surface area); (b) on the hip of L variants (8 m^2 surface area).

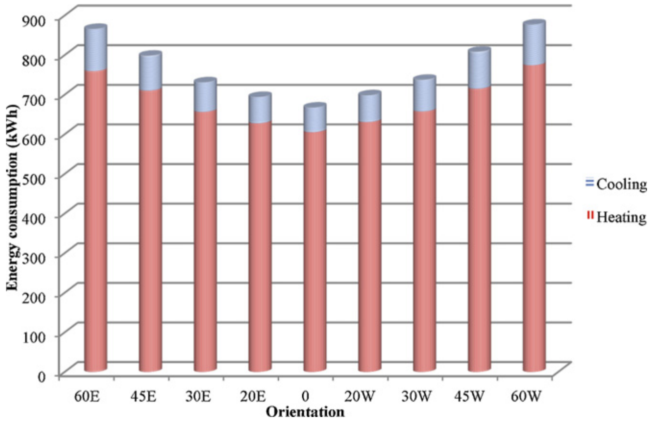

Fig. 7. Annual heating and cooling consumption (kWh) of the rectangular unit with different orientations.

cooling demand of west rotated units is slightly larger than for east rotated units.

Results for non-rectangular shapes indicate that L shape, L variant (V-WS30) and obtuse-angle shape require 7%, 6% and 2% respectively, more heating energy than the reference case (rectangle). The cooling load of L variant exceeds that of the reference case by 19% and the obtuse-angle and L shape by 8% and 4%, respectively. Cooling and heating consumption of all L variants, computed using a heat pump with COP of 4, is shown in Fig. 8.

3.2.2. Density

3.2.2.1. Comparison between units in isolation and in assemblage. The arrangement of units with respect to each other in a site can result in mutual shading. An additional effect is the orientation of individual units. To isolate the adjacency effect from the effect of orientation in curved site layouts, only the central due south unit in a site is compared to the corresponding isolated unit. The results indicate that in general, the heating load increases for detached units in a neighborhood while cooling load decreases, as compared to the corresponding isolated units (Fig. 9). The increase in heating load reaches 12% and 22% for the rectangular shape in site I and site II, respectively. L shape heating load increases by 15% in site II as compared to 12% in site I. One reason for this effect is the shade cast on the east and west facades, in all configurations, and partially on south-facing facades in sites II and III.

3.2.2.2. Effect of spacing. Energy demand for heating and cooling of attached units is lower than for the corresponding detached configurations. For instance, heating demand of the attached rectangles and attached obtuse-angle configurations is reduced by 35% and 20% respectively, relative to the detached units. The average values of heating demand for units of each site, corresponding to the spacing values (attached A – s_0, detached D – s_1, and 2D – s_2) are shown in Fig. 10. For site I, only configurations of the rectangular shapes and of L variants are shown in Fig. 10, since obtuse-angle is not studied for this site.

Doubling the space between the units (from s_1 to $s_2 = 2s_1$), does not affect significantly the heating demand; however the cooling load increase with larger spacing between units. Energy used for cooling is negligible as compared to that required for heating (ca. 10% of heating demand).

For all shapes, heating demand is lower in site I than in the two other sites, and in site II they are lower than in site III.

3.2.3. Row effect

The row effect on heating and cooling loads is assessed for site I by comparing the loads of obstructed and exposed rows to the corresponding isolated row. The results of this comparison are presented in Fig. 11a and b for detached and attached units respectively. The results indicate that generally, the average heating load increases significantly for the units of the obstructed row (R2), while the cooling load decreases. For the exposed row (R1), heating and cooling load are affected for a row spacing of 10 m or less. The heating load of the obstructed row of detached rectangular units (Fig. 10a) increases by ca. 50% at 5 m row spacing and by 25% at 10 m spacing. The corresponding values for the exposed row are 15% and 5% respectively. For attached rectangular units (Fig. 11b), the increase of the heating load of the obstructed row is about 70% at 5 m row spacing and 30% at 10 m spacing. At 20 m there is no significant effect.

For L variant, the exposed row is not affected, while the obstructed row of detached units requires 25% more heating at 5 m spacing, and 10% at 10 m. The attached units of L variant in the obstructed row require 35% more heating at 5 m, and 15% at 10 m spacing.

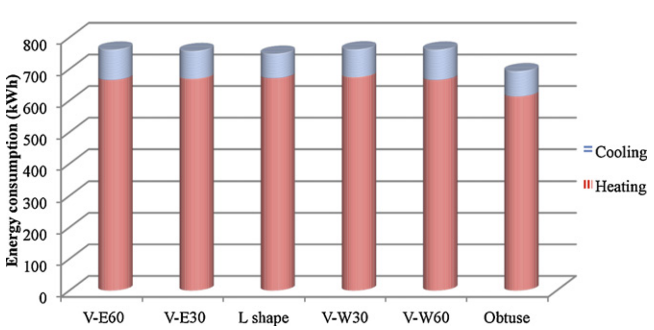

Fig. 8. Annual heating and cooling of L and L variant shapes.

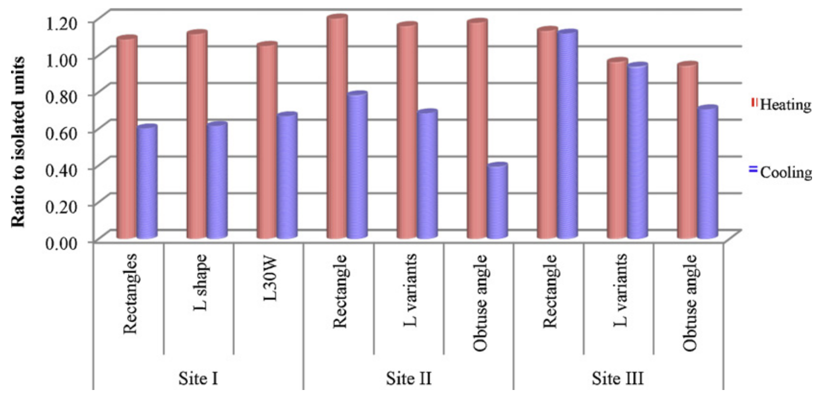

Fig. 9. Comparison of heating and cooling demand between isolated units and detached units in a neighborhood.

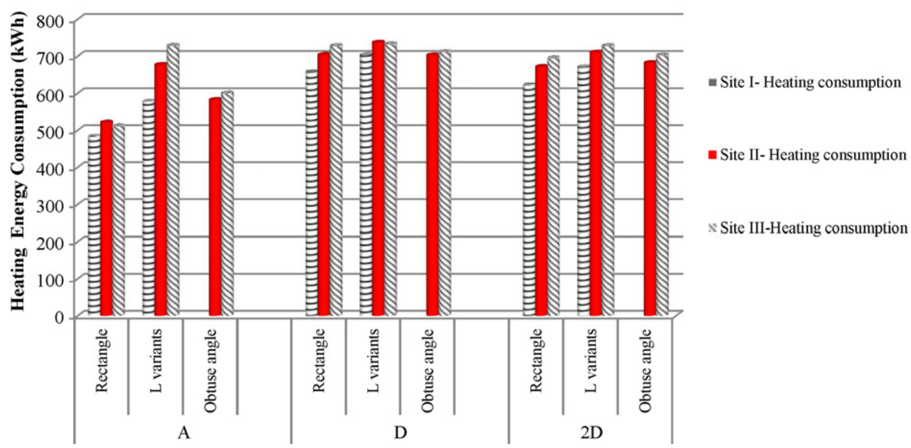

Fig. 10. Heating consumption at different spacing between units in site II and site III.

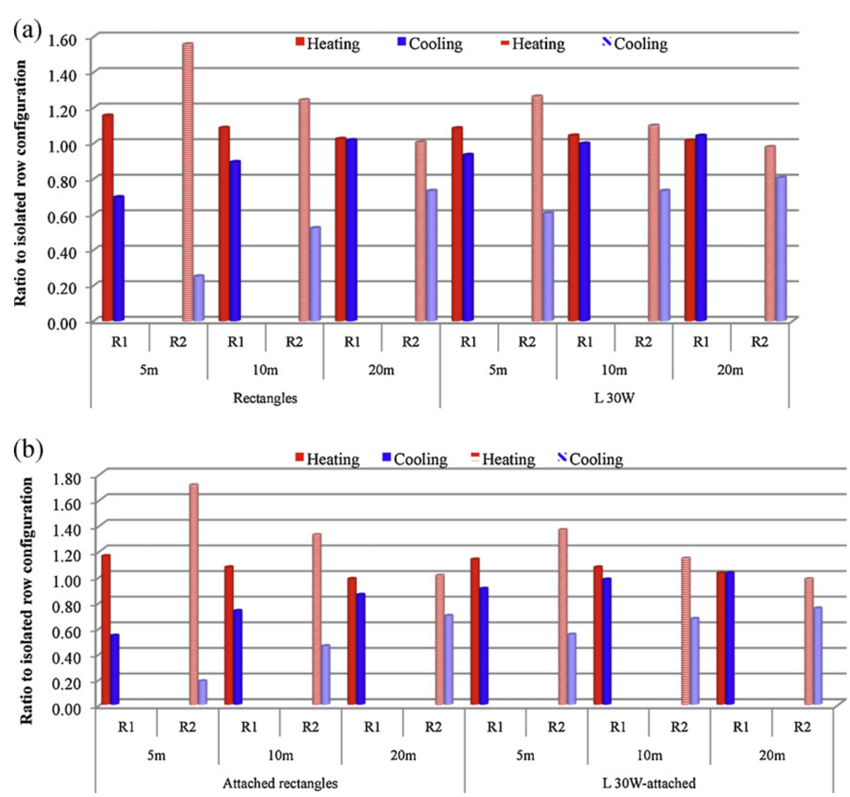

Fig. 11. Comparison of the row effect in site I–R1 exposed row, R2 obstructed row: (a) Detached configurations, (b) attached configurations.

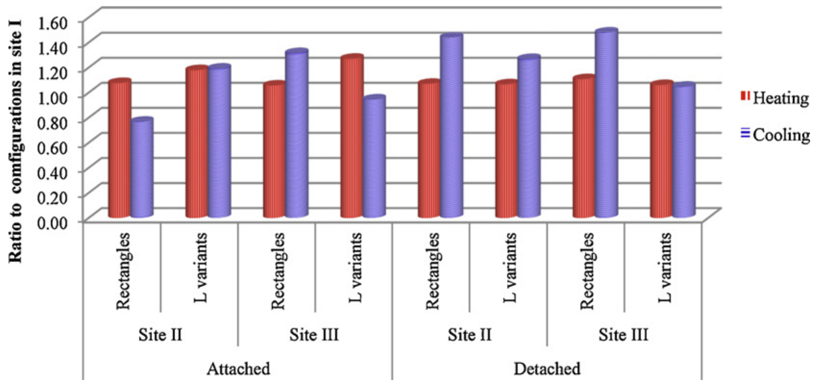

Fig. 12. Heating and cooling loads of sites II and III relative to site I.

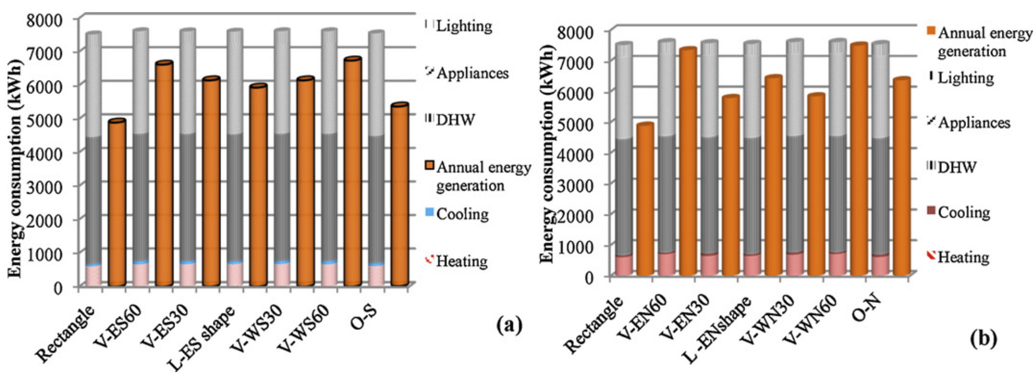

Fig. 13. Energy demand and production for isolated units of different shapes: (a) shapes of sites I and II; (b) shapes of site III.

3.2.4. Site effect

The effect of site layout on energy demand is analyzed by comparing configurations of rectangular and L variant shapes in site II and site III to the corresponding configurations in site I. The results are presented in Fig. 12. For detached configurations only the cooling load increases in site II and III (Fig. 12). For instance, the cooling load of the rectangular configurations is increased by approximately 45% and 48% for site II and site III respectively. However, the energy consumption for cooling is low (average of 55 kWh, for the rectangular configuration in site II). One important reason for the increase of cooling load in site II and site III, is the fact that all rectangular units have the same south-facing window area, which, when the units are rotated, become near west or east facing, resulting thus by increased transmitted radiation in the morning and the evening, when the sun is at low altitude during the summer period. This can be resolved by modifying the window area, for the rotated units.

In the attached configurations, the heating load of L variants in site III is 25% higher than in site I. This can be explained by the shade cast on several south facades of this configuration. The attached rectangle configuration requires 8% and 6% more heating for site II and III respectively.

3.3. Evaluation of energy balance

In this section energy demand and supply are compared for the different configurations studied.

3.3.1. Isolated units

The total consumption of electricity for lighting, DHW and appliances, in addition to the computed heating and cooling energy consumptions, for isolated units of each shape is presented in Fig. 13 alongside the energy production of the corresponding units. The rectangle with gable roof (optimum roof – not shown in Fig. 13) produces some 2% more than it consumes. By contrast, electricity production of the reference rectangular layout with hip roof is some 35% less than consumption. Some L variants, such as V-EN30W, produce up to 96% of total consumption. The results in terms of percentage of energy production to energy production of all shapes are presented in Table 5.

3.3.2. Neighborhoods

Total energy supply/demand balance for assemblages in all sites are presented in Table 6. Following are the main observations:

Table 5
Ratio of energy production to consumption.

Shapes/site II and site I	Rectangle/gable roof	Rectangle	V-ES60	V-ES30	L-ES	V-WS30	V-WS60	O-S
Ratio of energy generation to energy use	1.02	0.65	0.87	0.81	0.78	0.81	0.89	0.71
Shapes/site III		Rectangle	V-EN60	V-EN30	L-EN	V-WN30	V-WN60	O-N
Ratio of energy generation to energy use		0.65	0.94	0.74	0.83	0.74	0.96	0.81

Table 6
Ratio of energy production to total energy consumption of all configurations.

	Ratio of energy generation to energy use for all the neighborhood							
Site	Site I		Site	Site II		Site III	
DensityShape	Detached	Attached	DensityShape	Detached	Attached	Detached	Attached
Rectangle	0.65	0.66	Rectangle	0.62	0.58	0.63	0.70
L shape	0.74	0.75	L variants	0.81	0.81	0.85	0.82
L variants	0.79	0.79	Obtuse	0.74	0.73	0.75	0.85

- Configurations of L variants, in both site I and site II generate around 80% of their total energy consumption.
- In site III, L variant shape is optimal for detached configuration while the obtuse-angle is optimal for the attached configuration. These configurations generate 85% of the total energy consumptions (Table 6).
- In site I, L variants can supply 79% of the total energy need, while the rectangular configuration generates ca. 65%.

4. Conclusion

This study evaluates housing neighborhoods characterized by the shape of housing units and their density and by the layouts of the sites in which these neighborhoods are located. The potential of these neighborhoods to generate electricity is compared with energy demand. The study assumes design strategies for solar energy houses and energy demand data as proposed in the literature for mid-latitude locations (Montreal, Canada).

Housing units considered in this study are two-storied with a total floor area of 120 m^2. Housing units' shapes include, in addition to rectangle, which serves as a reference, L shapes with varying values of the angle enclosed by the wings. The three site layouts considered are straight road, south-facing semi-circular road and north-facing semi-circular road. Housing density is considered trough detached configurations as lower density and attached configurations as higher density. Effect of rows of housing units is also considered for the straight road site. EnergyPlus building simulation program is used for estimating energy generation and demand. The main results of this study are discussed in the following.

4.1. Energy generation

- BIPV electricity production of roofs with a given tilt angle is affected primarily by the area of near-south facing roof surfaces, shade and orientation. Active roof area is largely affected by the shape of the housing units. Some shapes, such as in L variations, allow optimizing roof area for a given floor area. For instance total annual energy generation can be increased by up to 50% relative to the rectangular shape. This can be even more beneficial on a neighborhood scale, where the total electricity generation by the neighborhood can be significantly increased.
- The density effect is analyzed by studying attached units versus detached units, and analyzing the effect of row configurations. Attaching the units in multiplex configurations has the effect of increasing total active roof surface in some configurations. On the other hand it may produce some mutual shading by some configurations of L. The row effect does not have significant effect on electricity generation for a row distance larger than 5 m, in this study due to the uniform height of all units. A maximum reduction of 7% is observed for a 5 m row distance.
- The effect of site layout on electricity generation is mainly due to its interaction with the housing shape design. A favorable combination of shapes and layout can result in significant increase of energy production. For instance, L variant configurations, employed around a curved road, can yield up to 33% more electricity generation than the rectangular configuration, used in the same layout
- Another effect, resulting from variation in orientation of units in a curved layout is a shift in peak generation time by roof surfaces of differing orientations. A difference as large as 6 h of peak generation of different units can be achieved in a specific site layout. Shift of peak production can be beneficial for matching grid requirements.

4.2. Energy consumption for heating and cooling

- Deviation of shape from the rectangle, which is considered the optimal shape for energy demand, generally involves increase in heating load. A typical value of increased heating load is in the range of 2–8%. The increase of heating load of non-rectangular shapes is associated with decrease of the solar gain in winter due to mutual shading by wings, and their rotation relative to south, as well as with the increased area of the building envelope for a given floor area. Cooling load is also affected by increase of solar radiation on the rotated wings and by the large envelope area.
- Heating and cooling loads depend strongly on unit density in a site. Attaching units in multiplexes reduces heating loads by up to 30% and cooling load by up to 50% compared to the detached configurations of the same site. Heating and cooling loads of detached units are not highly sensitive to the spacing of the units.
- Arranging the units in south-facing rows affects significantly the obstructed row, due to shading. The heating load is inversely related to the distance between rows, while the cooling load of both exposed and obstructed rows is significantly lower than for the single row configuration. For instance with a distance of 10 m between rows, the heating load of the obstructed row can increase by up to 25% for the rectangular units. At 20 m distance the effect is negligible.
- Units in curved layouts have generally larger heating and cooling loads than in a straight road configuration. For instance, the increase in heating load of some L variants is up to 25% in some configurations of north-facing curve and 18% for south-facing curve. For the rectangular configuration the increase of heating load is some 8% for attached units and 11% for detached units, in both curved layouts. One reason of the increase of loads in curved roads is the mutual shade of the units, as for instance in north-facing curve, where L variants shade significantly each other. This shade can be reduced by more careful design of the relative ratio of self-shading surfaces. Cooling load is increased since the units are originally designed to be south-facing, implying large window size on the south facades. In the curved layouts, some of these units are oriented towards west or east, resulting in increasing transmitted radiation in the mornings and evenings, when the sun is at low altitude during the summer period.

4.3. Balance between electricity generation and electricity use

- In attempting to achieve a balance between energy demand and energy production it should be noted that heating and cooling demand constitute no more than 10–15% of total energy demand, when energy efficient heat pump is used. The rest of energy consumption is attributed to appliances, water heating and other items that are not affected by parameters considered in this study. The main objective, therefore, is to maximize electricity production, even at the expense of some increase in heating and cooling load.

- The general comparison between energy consumption, assuming energy efficient measures, and the energy production, show that several unit shapes included in this study are very close to achieve net zero energy status. For instance the units of L variants can produce up to 96% of their energy use, while the rectangular shape with hip roof (reference case) produce some 65% of the energy use. The rectangle with a gable roof (optimal roof), on the other hand, produces about 2% more than its energy use. Manipulation of roof design can help in improving production/consumption ratio. Multi-faceted roofs such L and its variants, in addition to increasing production associated with increased surface area, produce several peaks of generated electricity, due to the different orientations of surfaces.
- Some of the studied neighborhood configurations constitute near net zero energy communities. For instance the detached L variants and attached obtuse-angle of the north-facing curved site produce 85% of their energy consumption. The attached rectangular (trapezoid) configuration of the same site produces 70% of its total energy consumption. Additional measures can be taken to lower energy use for domestic hot water and space heating by implementing technologies such as hybrid thermal/photovoltaic systems.

5. Concluding remarks

The investigation presented in this paper forms part of a research program whose objectives include the development of an integrated design methodology for residential neighborhoods that takes into account energy efficiency consideration from the earliest stages of the design process. While the specific study presented is applicable to mid-latitude climates, the methodology is applicable to any climate, with some modifications to the basic design assumptions required to address specific climate conditions.

This investigation shows that a variety of housing unit shapes, densities and site layouts can be accommodated in ways that compensate for increased energy consumption by increased generation, as well as by spread of peak generation timing. It is recommended that approach and simulation procedures employed in this study should be incorporated in the design process for energy efficient neighborhoods *ab-initio*.

Acknowledgments

The first author would like to thank the Natural Sciences and Engineering Research Council of Canada (NSERC) for its financial support through a CGS D2 Alexander Graham Bell Graduate Scholarship. Support was also received from NSERC discovery grants held by Drs Andreas Athienitis and Paul Fazio. This work was also partly supported by the NSERC Smart Net-zero Energy Buildings Strategic Research Network.

References

[1] P.A. Torcellini, D.B. Crawley, Understanding zero-energy buildings, ASHRAE Journal 48 (9) (2006) 62–64, 66–69.
[2] V. Karsten, M. Riley, IEA Joint Project: Towards Net Zero Energy Solar Buildings (NZEBs), IEA SHC Task 40 – ECBCS Annex 52, 2009.
[3] M. Cellura, G. Ciulla, V. Lo Brano, A. Orioli, L. Campanella, F. Guarino, D. Nardi Cesarini, The redesign of an Italian building to reach net zero energy performances: a case study of the SHC Task 40 – ECBCS Annex 52 (ML-11-C040), ASHRAE Transactions 117 (Part 2) (2011).
[4] ASHRAE, Solar Energy Use, ASHRAE Handbook HVAC Applications, ASHRAE, Atlanta, GA, 2007 (Chapter 33).
[5] S. Pelland, Y. Poissant, An evaluation of the potential of building integrated photovoltaics in Canada, in: 31st Annual Conference of the Solar Energy Society of Canada (SESCI), August 20–24th 2006, Montreal, Canada, 2006.
[6] I.E.A., Potential for building integrated photovoltaics, Technical Report IEA – PVPS T7-4, 2002.
[7] J.A. Duffie, W.A. Beckman, Solar Engineering of Thermal Processes, Wiley, 2006, p. 928.
[8] M. Buresch, Photovoltaic Energy Systems, McGraw-Hill Book Company, 1983.
[9] W.H. Kemp, The Renewable Energy Handbook: A Guide to Rural Energy Independence, Off-Grid and Sustainable Living, Aztech Press, Tamworth, ON, 2006.
[10] J.D. Mondol, Y.G. Yohanis, et al., The impact of array inclination and orientation on the performance of a grid-connected photovoltaic system, Renewable Energy 32 (1) (2007) 118–140.
[11] C. Hachem, A. Athienitis, P. Fazio, Parametric investigation of geometric form effects on solar potential of housing units, Solar Energy (2011), doi:10.1016/j.solener.2011.04.027.
[12] C. Hachem, A. Athienitis, P. Fazio, Design of solar optimized neighbourhood, in: ASHRAE 2011 Annual Conference, June 25–29th, Montreal, Canada, 2011.
[13] D. Chiras, The Solar House: Passive Heating and Cooling, Chelsea Green Publishing, White River Junction, VT, 2002.
[14] J.P. Kim, Land-use Planning and The Urban Heat Island Effect Dissertation City and Regional Planning, The Ohio State University, 2009.
[15] K. Steemers, Energy and the city: density, buildings and transport, Energy and Buildings 35 (1) (2003) 3–14.
[16] R.L. Knowles, Sun Rhythm Form, The MIT Press, Cambridge, Massachusetts, 1981.
[17] A. Okeil, A holistic approach to energy efficient building forms, Energy and Buildings 42 (2010) 1437–1444.
[18] M.J. Leveratto, Urban planning instruments to improve winter solar access in open public spaces, Environmental Management and Health 13 (4) (2002) 366–372.
[19] T.N. Stasinopoulos, Sunny walls vs. sunnier roofs: a study on the advantages of roofs for solar collection, Environmental Management and Health 13 (4) (2002) 339–347.
[20] R. Compagnon, Solar and daylight availability in the urban fabric, Energy and Buildings 36 (4) (2004) 321–328.
[21] J.H. Kampf, M. Montavon, J. Bunyesc, R. Bolliger, D. Robinson, Optimisation of buildings' solar irradiation availability, Solar Energy 84 (2010) 596–603.
[22] C. Hachem, A. Athienitis, P. Fazio, Investigation of solar potential of housing units in different neighborhood designs, Energy and Buildings (2011), doi:10.1016/j.enbuild.2011.05.008.
[23] Center for Watershed Protection (CWP), Better Site Design: A Handbook for Changing Development Rules in Your Community, Ellicott City, MD, 1998.
[24] A. Cohen, Narrow streets database, Congress for the New Urbanism (2000), www.sonic.net/abcaia/narrow.htm.
[25] D. Burden, M. Wallwork, K. Sides, H. Bright, Street design guidelines for healthy neighborhoods, Rue for Local Government Commission Center for Livable Communities (1999).
[26] J. Teed, P. Condon, S. Muir, C. Midgley, Sustainable urban landscape neighbourhood pattern typology, The University of British Columbia James, Produced for the Sustainable Development Research Institute, 2009.
[27] EnergyPlus, Version 5, Lawrence Berkeley National Laboratory, Berkeley, CA, 2010.
[28] A.K. Athienitis, M. Santamouris, Thermal Analysis and Design of Passive Solar Buildings, James & James Ltd., London, 2002.
[29] A. Athienitis, Design of a solar home with BIPV-thermal system and ground source heat pump, in: 2nd Canadian Solar Buildings Conference, June 10–14, Calgary, Canada, 2007.
[30] M. Armstrong, M.C. Swintona, H. Ribberink, I. Beausoleil-Morrison, J. Millette, Synthetically derived profiles for representing occupant-driven electric loads in Canadian housing, Journal of Building Performance Simulation 2 (1) (2009) 15–30.
[31] CMHC, Tap the Sun: Passive Solar Techniques and Home Designs, Canada Mortgage and Housing Corporation, Ottawa, 1998.
[32] Natural Resources Canada (NRCan), Heating and Cooling with a Heat Pump, Office of Energy Efficiency (OEE), 2008, http://oee.nrcan.gc.ca/publications/infosource/pub/home/heating-heat-pump/booklet.pdf, visited on 17 April 2011.
[33] I. Sartori, J. Candanedo, S. Geier, R. Lollini, F. Garde, A. Athienitis, L. Pagliano, Comfort and energy efficiency recommendations for net zero energy buildings, in: EuroSun Conference, Graz, Austria, 28th September–1st October, 2010.
[34] S. Pogharian, et al., Getting to a net zero energy lifestyle in Canada: the Alstonvale net zero energy house, in: 3rd European PV Solar Energy Conference, Valencia, Spain, 2008.
[35] EN 15316-3-1, Heating systems in buildings – method for calculation of system energy requirements and system efficiencies. Part 3-1. Domestic hot water systems characterisation of needs (tapping requirements), 2007.
[36] R. Charron, Development of a genetic algorithm optimisation tool for the early stage design of low and net-zero energy solar homes, Unpublished Ph.D. Thesis, Concordia University, 2007.
[37] C. Hachem, A. Athienitis, P. Fazio, Design of Roof Shapes for Increased Solar Potential of BIPV/T Systems, ISES, Kassel, Germany, August 28, 2011.

[38] National Research Council Canada: Institute if or Research in Construction (NRC-IRC), CBD-59, Principles of Solar Shading, 2005, http://www.nrc-cnrc.gc.ca/eng/ibp/irc/cbd/building-digest-59.html, visited on November 29, 2010.
[39] Google SketchUp Plugins, 2011. http://sketchup.google.com/intl/en/download/plugins.html.
[40] The weather network, http://www.theweathernetwork.com/statistics/degreedays/cl7025250, visited on November 2010.
[41] T. Hong, S.K. Chou, T.Y. Bong, A design day for building load and energy estimation, Building and Environment 34 (1999) 469–477.
[42] EnergyPlus, weather files, 2010, http://apps1.eere.energy.gov/buildings/energyplus/weatherdata_sources.cfm#CWEC, visited on 17-03-2010.
[43] ASHRAE, Fundamentals Handbook, Fenestration, American Society of Heating, Refrigerating, and Air-Conditioning Engineers (ASHRAE), 2005 (Chapter 31).
[44] P.G. Loutzenhiser, H. Manz, et al., Empirical validation of models to compute solar irradiance on inclined surfaces for building energy simulation, Solar Energy 81 (2) (2007) 254–267.
[45] P.G. Loutzenhiser, H. Manz, et al., An empirical validation of window solar gain models and the associated interactions, International Journal of Thermal Sciences 48 (1) (2009) 85–95.
[46] B.T. Griffith, P.G. Ellis, Photovoltaic and solar thermal modeling with the EnergyPlus calculation engine, in: World Renewable Energy Congress VIII and Expo Denver, Colorado, August 29–September 3, 2004.
[47] Natural Resources Canada (NRCan), Photovoltaic Potential and Solar Resources Maps of Canada, Natural Resources Canada, 2007, Retrieved February 1, 2011, from https://glfc.cfsnet.nfis.org/mapserver/pv/rank.php?NEK=e.